Nonlinear Processes in Geophysics (1996) 3: 77–88

Nonlinear Processes in Geophysics

Manifestation of nonlinear elasticity in rock: convincing evidence over large frequency and strain intervals from laboratory studies

P. A. Johnson*[1], P. N. J. Rasolofosaon[2]

[1]Los Alamos National Laboratory, Los Alamos, New Mexico
[2]Institut Français du Pétrole, Rueil Malmaison Cedex, France

*Also at Department d'Acoustique Physique, Université Pierre et Marie Curie (Paris 6)

Received 15 June 1995 - Accepted 9 October 1995 - Communicated by D. Sornette

Abstract. Nonlinear elastic response in rock is established as a robust and representative characteristic in rock rather than a curiosity. We show measurements of this behavior from a variety of experiments on rock taken over many orders of magnitude in strain and frequency. The evidence leads to a pattern of unifying behavior in rock: (1) Nonlinear response in rock is ubiquitous. (2) The response takes place over a large frequency interval (dc to 10^5 kHz at least). (3) The response not only occurs, as is commonly appreciated, at large strains but also at small strains where this behavior and the manifestations of this behavior are commonly disregarded.

1 Introduction

Studies of nonlinear response of rock show that in contrast to most solids, the nonlinear response in rock is strikingly large, orders of magnitude larger than most solids (e.g., Birch, 1966; Bakulin and Protosenya, 1981; Zinov'yeva et al., 1989; Ostrovsky, 1991). The observations are robust in that they take place over many orders of magnitude in both frequency and strain, as will be illustrated here. Nonlinear response in the context of static stress-strain measurements is neither new nor novel; however, the realization that nonlinear behavior exists at even moderate strains is not commonly appreciated.

Our intention is to describe several manifestations of nonlinear behavior in rock. Nonlinear response may manifest itself in a variety of manners, including a nonlinear stress strain relation, nonlinear attenuation, harmonic generation and resonant peak shift, all of which are related (e.g., Winkler et al., 1979; Bakulin and Protosenya, 1981; Johnson et al., 1987;1989; Nazarov et al., 1988; Zinov'yeva et al., 1989; Ostrovsky, 1991; 1993; Beresnev and Nikolaev, 1988; Bonner and Wanamaker, 1991; Murphy, 1982; Liu, 1994; Johnson et al., 1996). Figure 1 illustrates the frequency and strain intervals of experiments described in this paper. The experiments include: static stress-strain tests on rock that are conducted over strain intervals of 10^{-1} to 10^{-4} and frequencies of near dc to 1 Hz where the modulus is obtained from the stress-strain derivative (I in Figure 1); torsional oscillator experiments that are conducted over strain intervals from 10^{-4} to 10^{-7} and frequencies of 0.1 to 100 Hz (II in Figure 1); resonant bar experiments that take place over strain intervals of 10^{-4} to 10^{-8} and intervals in frequency from 10^2 to 10^4 Hz (III in Figure 1); and dynamic, propagating wave experiments that are conducted at strain levels of 10^{-6} to 10^{-9} and frequencies of 10^3 to 10^6 (IV in Figure 1).

Each type of experiment is used to interrogate the nonlinear response of a sample in a different manner. The static tests are whole-volume experiments in contrast to the other experiments. The dynamic experiments preferentially interrogate portions of the sample in different manners. For example, the torsional experiments preferentially sample the outer radial portion of the sample; the resonance experiments preferentially sample the bar center. However, we believe that the responsible mechanism for nonlinear response (to first order) is always the same: the presence of compliant features and the influence of fluid (e.g., see Gist, 1994). We define compliant features as those features that are the weakest in the rock, e.g., grain-to-grain contacts, low aspect ratio cracks, joints, etc. In addition, there may be other mechanisms responsible as yet unidentified.

The first portion of this paper briefly describes classical theory. The second portion of the paper describes experiments, apparati, and results. This second portion is divided into sections describing the four types of experiments mentioned above and the corresponding experimental results. Section 3.1 describes static results; section 3.2 describes torsional oscillator results; section 3.3

Correspondence to: P. A. Johnson

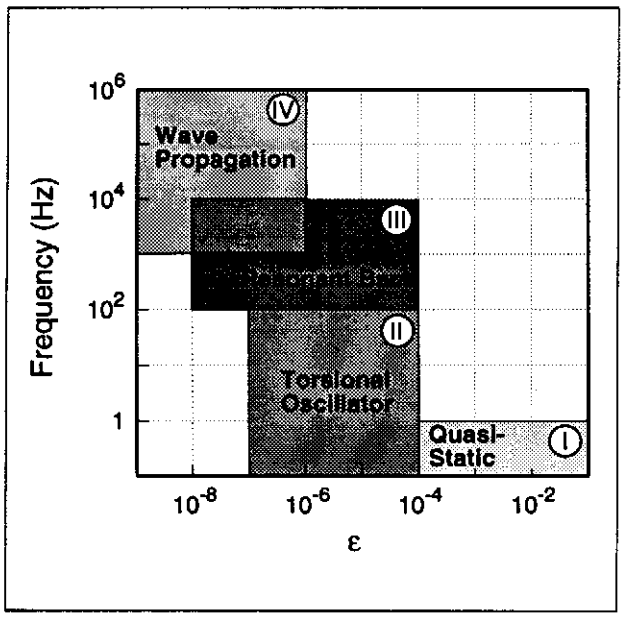

Fig. 1. A graphic representation of the frequency and strain intervals over which observation of nonlinear response in rock are observed and described in this paper.

describes resonant bar studies; and section 3.4 describes dynamic, pulse mode studies. Following this there will be a brief discussion and conclusions. This paper is not meant to be an exhaustive review of published experimental results from all available sources. Rather, we emphasize the robust nature of observations by illustrating several examples. In addition, we do not review the related theoretical results. These can be found in Landau and Lifshitz (1986) and papers by Ostrovsky (1991); McCall (1993); and Guyer et al. (1995a), among others. Finally, we do not present nonlinear parameters derived from these experiments as our purpose is to illustrate rather than quantify nonlinear response.

2 Classical Theory

We describe the basic theory only so that an understanding of what is meant by nonlinear elasticity is clear. It is not our intention to provide a review of companion theory and therefore we only mention the classical description of nonlinear elasticity.

In the approach of Landau and Lifshitz, nonlinear elasticity implies a perturbation expansion of the modulus or velocity in terms of the strain $(\partial u/\partial x)$:

$$c^2 = c_0^2[1 + \beta(\frac{\partial u}{\partial x}) + \delta(\frac{\partial u}{\partial x})^2 + ...], \quad (1)$$

where c is the perturbed wave speed, c_0 is the unperturbed wave speed, and β and δ are coefficients that characterize the cubic and quartic anharmonicities (they are the nonlinear moduli). Note that

$$c^2 = \frac{M}{\rho} \quad (2)$$

where M is modulus and ρ is the density. The expansion of velocity can be incorporated into the wave equation to describe nonlinear effects such as harmonics. Because the modulus is also the derivative of stress with respect to strain in the static case, the stress-strain relation also becomes nonlinear:

$$\sigma = M_0(\frac{\partial u}{\partial x})[1 + \beta(\frac{\partial u}{\partial x}) + \delta(\frac{\partial u}{\partial x})^2 + ...], \quad (3)$$

with $M_0 = c_0^2\rho$. It is important to note that this model has worked very well for ordinary materials that exhibit small nonlinear response. Rocks are far more complex and far more elastically nonlinear (hysteresis and end point memory– see below). A discontinuous model such as that described by Guyer et al. (1995a; 1995b, 1996) is an alternative and appears to be a more physically realistic approach (also see Nazarov et al., 1988; Kadish et al., 1996).

3 Experimental method, apparatus, and sample results

The following four sections illustrate experimental configurations and sample results for various experiments. Each type of experiment represents correspondingly decreasing strain intervals.

3.1 Static tests of stress-strain (strain range 10^{-1} to 10^{-4}, frequency range near dc to 1 Hz)

We illustrate experiments conducted by Hilbert et al. (1994). Many such data exist, but the experiments carried out by these researchers carefully explore the points we wish to emphasize here: nonlinearity in the stress-strain curve, hysteresis, end point memory (EPM), and nonlinearity in the modulus-stress curve from simultaneous time delay measurements. All are manifestations of elastic nonlinearity and are intimately related. We illustrate two experiments. The first experimental result illustrates the nonlinear response from a static test (nonlinearity in the stress-strain curve) and the second result illustrates velocity (modulus) versus stress obtained for the same experiment.

3.1.1 Stress - strain apparatus

The experimental apparatus used by Hilbert et al. (1994) is shown in Figure 2. In a typical experiment a rock sample is compressed uniaxially while radial strain is suppressed. The rock sample in this experiment is Berea sandstone with dimensions 42.4 mm long by 50.8 mm in diameter. The sample is pressurized from ambient conditions up to some predetermined maximum pressure while sample strain, axial and radial stress, and axial time delay are simultaneously monitored. Strain ϵ is

$$\frac{\Delta L}{L_0} \quad (4)$$

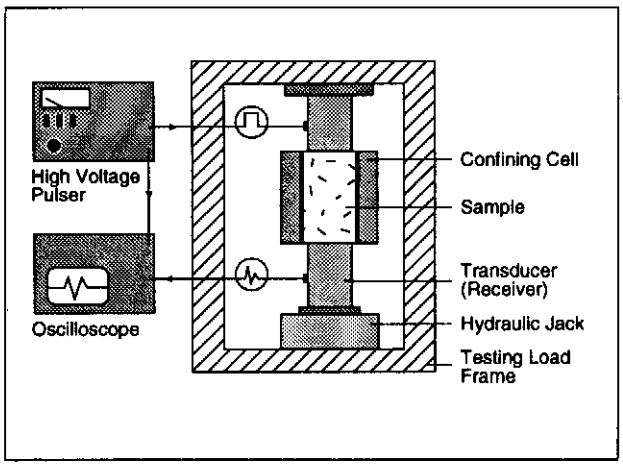

Fig. 2. Experimental apparatus for stress-strain and modulus-stress tests conducted by Hilbert et al. (1994).

where ΔL is the change in length of the sample and L_0 is the unperturbed length. In the experiment shown here, the sample was subjected to a maximum stress of 25 MPa and strain gauges were mounted longitudinally and radially around the entire diameter of the specimen for measurement of strain. Measurements were also made as stress was decreased in order to characterize the hysteresis of the material. The area within the hysteresis loop is a direct measurement of the energy loss over a cycle, and is also indicative of nonlinear response. By definition, attenuation

$$\frac{1}{Q} = \frac{\Delta E}{E} \tag{5}$$

where ΔE is the energy loss per cycle and E is the average energy per cycle (e.g., Toksöz and Johnston, 1981). Smaller stress-strain excursions are also carried out within the primary loop.

3.1.2 Experimental results

Figures 3 and 4 illustrate the stress time history (protocol) and the corresponding stress-strain response for the Berea sandstone sample, respectively. The purpose of the smaller excursions is to explore the effect of smaller stress-strain deviations at some ambient pressure. The velocity (modulus) was measured under the same stress conditions. The velocity result for the outer stress-strain loop from Figure 4 is shown in Figure 5. Velocity data were obtained from simultaneous measurement of pulse time delay with the outer cycle stress-strain data shown in Figure 4. Note that this plot illustrates that the material displays hysteresis in the dynamic velocity (modulus) as well.

A final point about Figure 4 is the so-called end point memory (EPM). EPM is illustrated by each of the small stress excursions in the figure. As illustrated in this figure, when the sample is taken to a given stress state, if the stress is slightly relieved but then is returned to

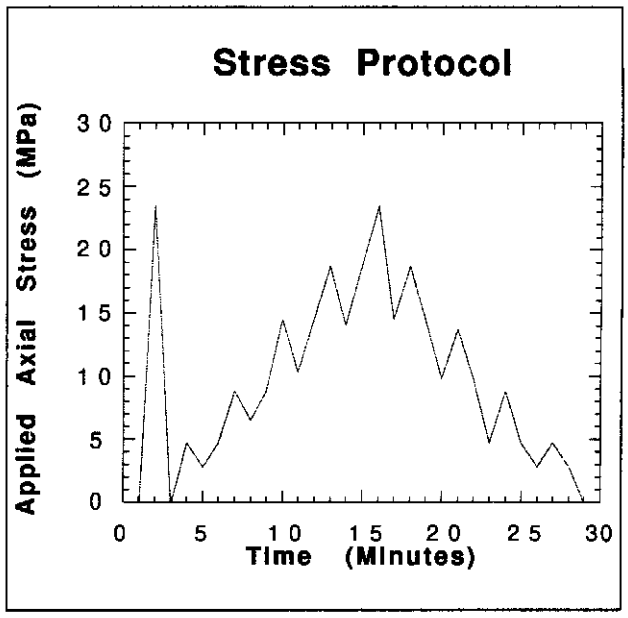

Fig. 3. Stress history or "protocol " for stress-strain data shown in Figure 4.

the previous stress, the rock will return to the previous strain level as well. In essence, the rock "remembers" its previous maximum strain level. This is an important property of rock related to the hysteresis and is discussed at length by McCall and Guyer (1994), Guyer et al. (1995a;1995b), and Guyer and McCall (1995).

The significant points we note from these experiments are, (1) the stress-strain relation and the modulus-stress relation are nonlinear, and thus the static and dynamic/static moduli are nonlinear; (2) hysteresis is characteristic of rocks; (3) end point memory is a property of rock; and (4) end point memory is a manifestation of nonlinearity as well.

3.2 Torsional oscillator experiments: strain range 10^{-4} to 10^{-7}, frequency range 10^{-1} to 10^{2} Hz

The torsional oscillator experiments described here demonstrate the effects of elastic nonlinear behavior over strain and frequency intervals of 10^{-4} to 10^{-7} and 10^{-1} to 10^{2} Hz, respectively. The experiments differ from those that follow in that the nonlinear response of the sample in torsion is measured rather than the Young's mode response. We believe that the manifestation of nonlinear response is due to the same mechanism that is responsible for nonlinear response at all scales and in all of the experiments described in this paper. That is, nonlinear response is due to the presence of compliant features and the contained fluid. Both flexing of compliant features and sliding at the grain-scale level are likely responsible in torsion.

The examples chosen for display here are three separate experiments. Experiment 1 shows the effects of increasing stress on the shear modulus G, a similar result to

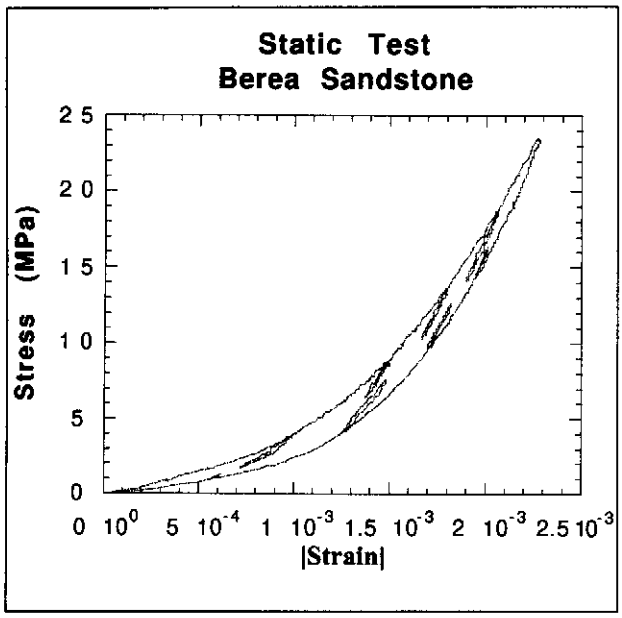

Fig. 4. Stress-strain curve from uniaxial quasi-static test for sandstone. The plot illustrates a nonlinear stress-strain relation, hysteresis, and end point memory.

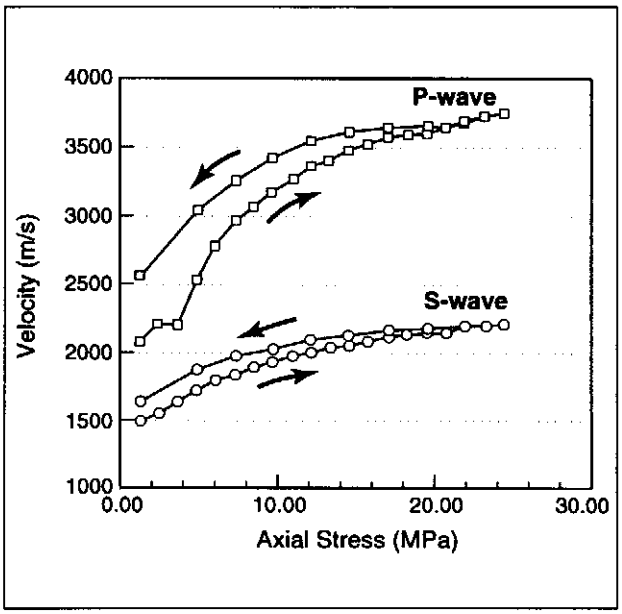

Fig. 5. Velocity (modulus) obtained while the rock is cycled through the outer cycle shown in Figure (4).

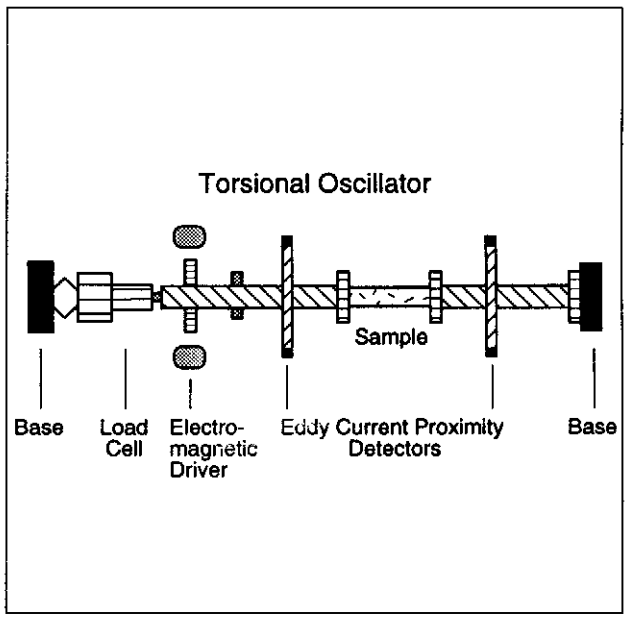

Fig. 6. Torsional oscillator apparatus.

that shown in the static test above. Experiment 2 shows the harmonic spectrum of the time series output from a separate experiment. Experiment 3 shows that introducing additional damage to a sample results in an additional elastically nonlinear response. Additional descriptions of these kinds of experiments can be found in Bonner and Wanamaker (1990;1991).

3.2.1 Torsional oscillator apparatus

The torsional oscillator apparatus is shown in Figure 6. The apparatus can be considered a segmented torsional spring with the drive end stationary. Torsion is measured along arms extending from the apparatus by use of eddy current proximity detectors configured to measure differential torsional displacement in the sample. The reference torsion is measured on aluminum by the proximity detector near the drive end (aluminum can be regarded as linear compared to the rock sample). The reference torque is compared to the torque at the other end of the rock sample and is measured with the second proximity detector. The shear modulus G can be computed from the difference in phase angle between the drive and the response of the sample using the two proximity detectors. The time signal can also be obtained at either end of the sample for harmonic analysis. A uniaxial load can be simultaneously applied for investigation of the effects of uniaxial stress.

In the following experiments, a 20 mm-long sample of Sierra White granite is oscillated in torsion over the range of strains from 10^{-4} to 10^{-7} at a frequency of 1 Hz. As the shear strain increases linearly with radius the method preferentially measures the effect away from the sample axis; however, for illustration torque is assumed to be distributed uniformly over the entire

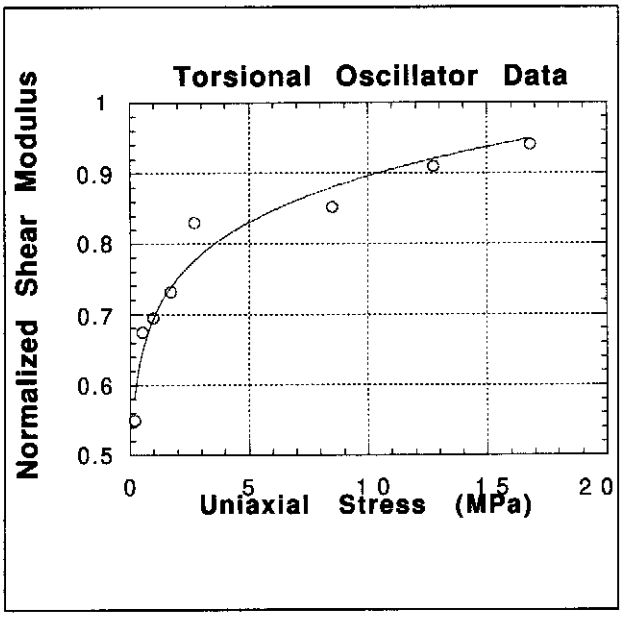

Fig. 7. Shear modulus G as a function of uniaxial load for maximum applied shear stress τ of 1 MPa in a sample of granite. G has been normalized to the value of the unfractured sample, G_{intact}. Measurements were made at 1 Hz.

sample for calculation of G. Nonlinear response is observed in the relation of shear modulus with stress, in harmonics, and in changes in the shear modulus when additional damage (compliant features) are introduced.

3.2.2 Experimental results

Experiment 1. In the experiment measuring G as a function of stress, additional cracks and a complete fracture were first induced in the sample by bending. This was done in order to make the sample more elastically nonlinear. The fractures were oriented perpendicular to the core axis. They were "mated" to their best fit after fracturing for the experiments. The sample was then preloaded with a normal stress of 0.1 to 0.2 MPa in order to hold the sample in place, and subsequently the stress is increased.

Figure 7 shows the results of shear modulus as a function of uniaxial stress for a maximum applied shear stress τ of 1 MPa. The modulus G has been normalized to the value before fracturing. The most important aspect of the result is that the behavior is similar to that of rock under static compression: the response of the rock is highly nonlinear, and becomes less so as the uniaxial stress is increased because more and more compliant features close. The result is similar for an unfractured sample but the nonlinear response is less intense.

Experiment 2. Figure 8 shows the power spectrum obtained from the time series output for several oscillations of applied torque. The plot shows the ratio of the power spectra for large to small levels of τ at two different applied uniaxial loads for an unfractured sam-

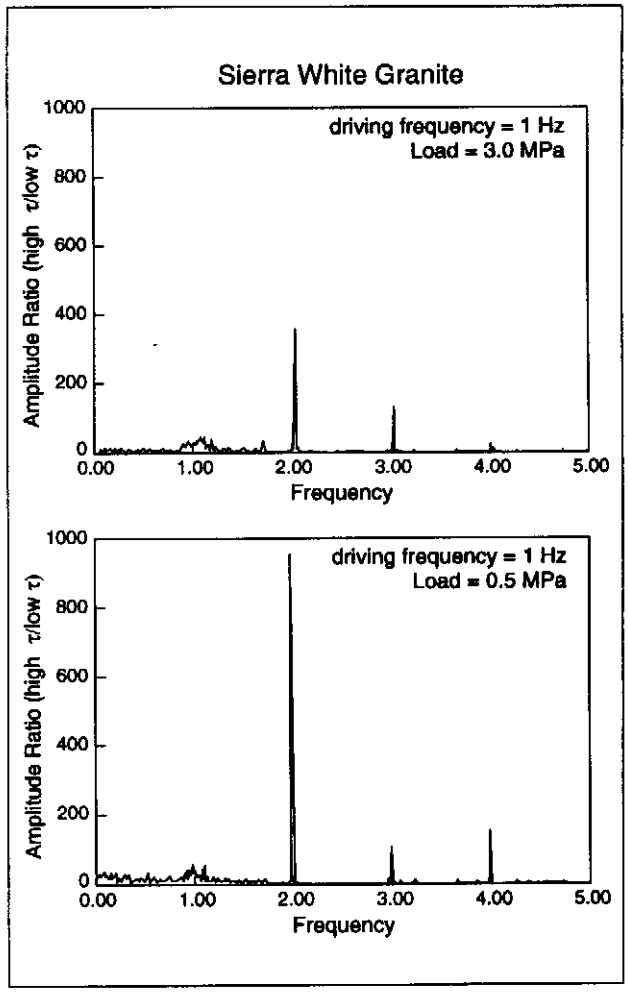

Fig. 8. Ratio of power spectra for large and small τ at two different applied uniaxial loads. The data were obtained from the time series of the sinusoidal output of the torsional oscillator experiment. Applied loads were 3.0 and 0.5 MPa for the top and bottom plots, respectively.

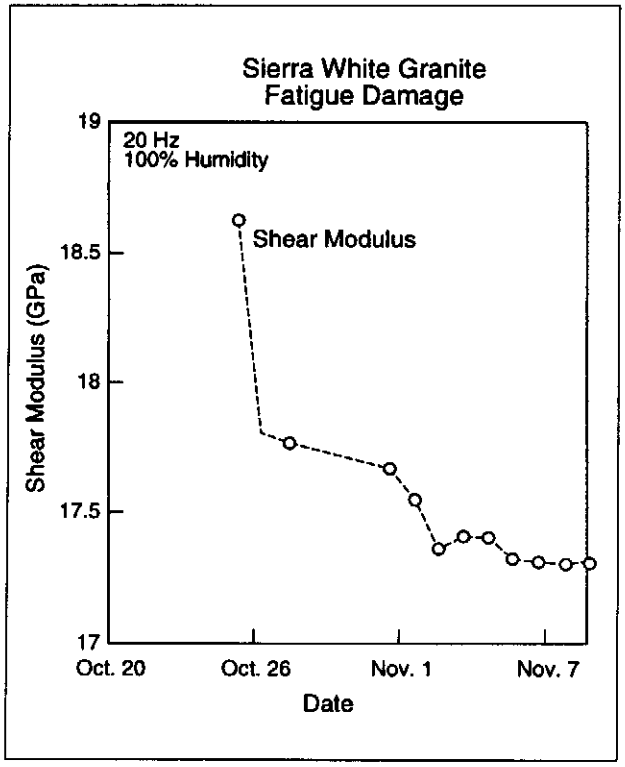

Fig. 9. Shear modulus monitored as a function of time while the sample was continually oscillated in the torsion apparatus.

ple of granite. The drive levels differ by approximately a factor of ten. Because the spectral ratios are plotted, the fundamental frequency at 1 Hz is very small. At low τ the harmonics are very small; however, at larger τ large harmonics appear. This is particularly true at small applied load (0.5 MPa). The second ($2f$), third ($3f$) and fourth ($4f$) harmonics are clearly observed. The effect becomes smaller for larger applied uniaxial stress (3 MPa) because more of the compliant features are locked.

Experiment 3. The final example from the torsional oscillator experiments is shown in Figure 9. In this experiment the shear modulus of an unfractured sample was monitored over a long period of time as the sample was progressively damaged, i.e., as more compliant features were induced by oscillation over a period of approximately 15 days. The experiment took place with a sample of granite at 100% relative humidity and at 20 Hz. The important point to note from this experiment is that as more damage is introduced, the modulus drops markedly.

The important points we wish to emphasize from the torsion experiments are as follows. (1) The modulus-stress relation is nonlinear. (2) Harmonics generated from the nonlinear response of the material are observed in torsion. (3) Damage induces a larger nonlinear response.

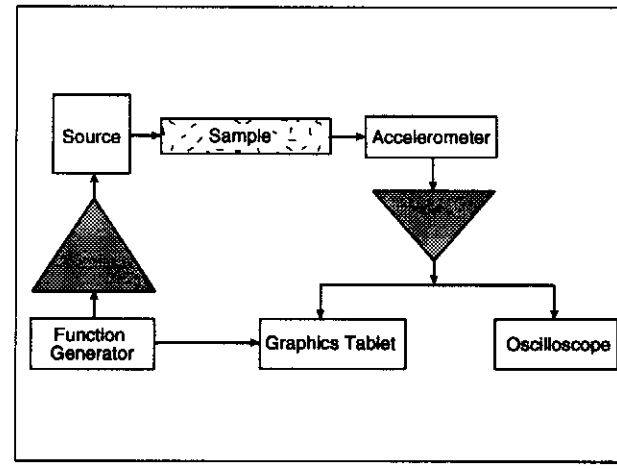

Fig. 10. Experimental configuration for resonant bar experiments.

3.3 Resonant bar experiments: strain range 10^{-4} to 10^{-8}, frequency range 10^2 to 10^4 Hz

The resonant bar experiments described here demonstrate the effects of elastic nonlinear behavior over strain and frequency intervals of 10^{-4} to 10^{-8} and 10^2 to 10^4 Hz respectively. The following describes comparative experiments between the relatively linear elastic material polyvinyl chloride (PVC) and a sample of Lavoux limestone. In these experiments, nonlinear elastic behavior is observed by measuring the response of the material in Young's mode resonance. Nonlinear behavior is manifested by resonant peak shift corresponding to a modulus shift, as a function of drive level. Independent confirmation of nonlinear behavior is inferred from observation of harmonics . A complete description of these and other results can be found in Johnson et al. (1996).

3.3.1 Resonant bar apparatus

The basic elements of the Young's mode experimental configuration for obtaining acceleration versus frequency measurements are shown in Figure 10. Measurements are made of both upward and downward swept frequency response over a chosen frequency interval. Typically, 5-20 frequency sweep experiments are repeated at successively increasing drive voltages over the same frequency interval in order to monitor resonant peak shift and harmonic generation. Acceleration is the parameter that is actually measured, but strain is of interest and can be directly calculated from the acceleration using the bar length (Johnson et al., 1996).

3.3.2 Comparison of PVC and rock under Young's mode resonance

Figure 11 shows a sample sequence of resonance curves for twelve different excitation levels in PVC, a material that is relatively "linear" in comparison with most rocks,

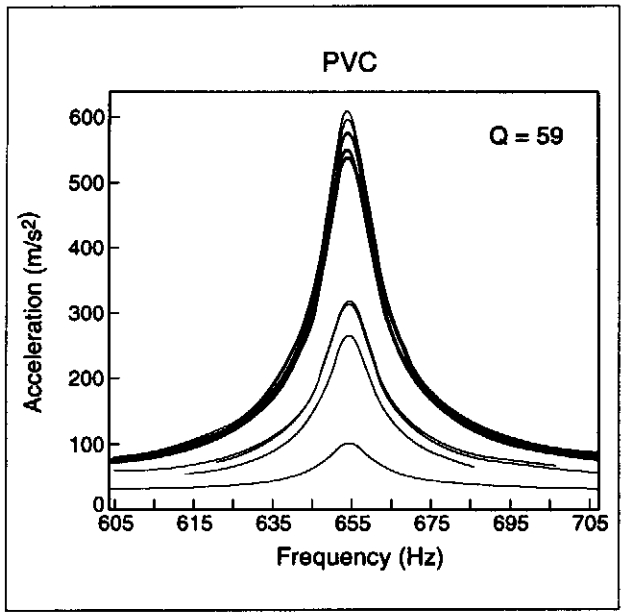

Fig. 11. Detected acceleration versus swept frequency for a sequence of resonance curves at twelve different excitation levels in polyvinyl chloride (PVC). Both downward and upward frequency sweeps are plotted. They are indistinguishable from each other.

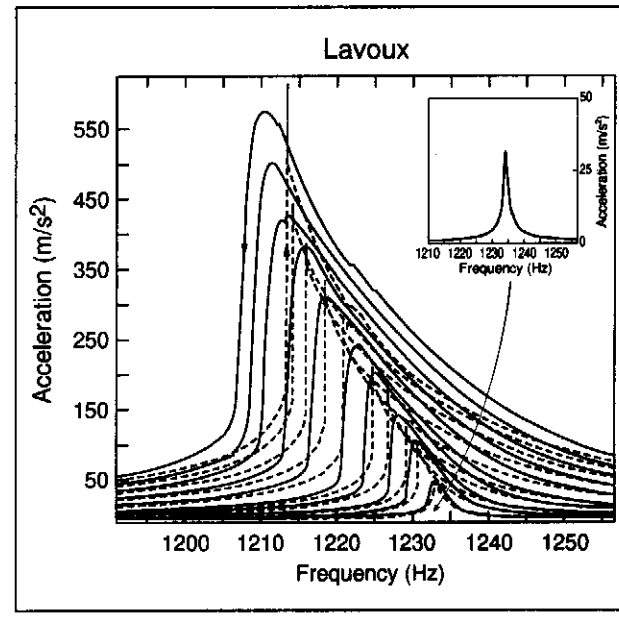

Fig. 12. Acceleration versus frequency for increasing excitation levels in Lavoux limestone at ambient conditions. The "linear" resonant peak is illustrated in the inset to show the character of the linear behavior at low drive level.

but with a similar Q to many rocks (Q = 59). The figure shows detected acceleration versus swept frequency. Both downward and upward resonant sweeps were conducted at each drive level but these are indistinguishable from each other. Within this acceleration/strain range, no harmonics are observed from the time signal.

Two observations from experiments with "linear" solids can be regarded as representative. (1) In general, these materials show no detectable change in resonance frequency with drive level (i.e., resonant peak bending); (2) If observed at all, higher harmonics are very weak when present over the acceleration/strain intervals detected (using a 12 bit digital oscilloscope and averaging signals).

In Figure 12, a representative result for Young's mode resonant behavior in rock is shown. The material is Lavoux limestone under ambient conditions. The solid lines represent downward frequency sweeps and the dashed lines represent upward frequency sweeps. Note also that the linear resonant response has been expanded vertically in Figure 12. Contrast this result to that of PVC shown in Figure 11. The difference is astonishing. Two observations are of note. First, the curve bending is dramatic as a function of detected acceleration in the rock. Second, the shape of the curve depends on the direction of the sweep, upward or downward in frequency. This second observation is typical of nonlinear oscillators in general (e.g., see Stoker, 1950). For a qualitative description of this behavior see Johnson et al. (1996).

The corresponding frequency spectrum illustrates the rich spectrum associated with large excitation level. Figure 13 shows two manifestations of nonlinear response

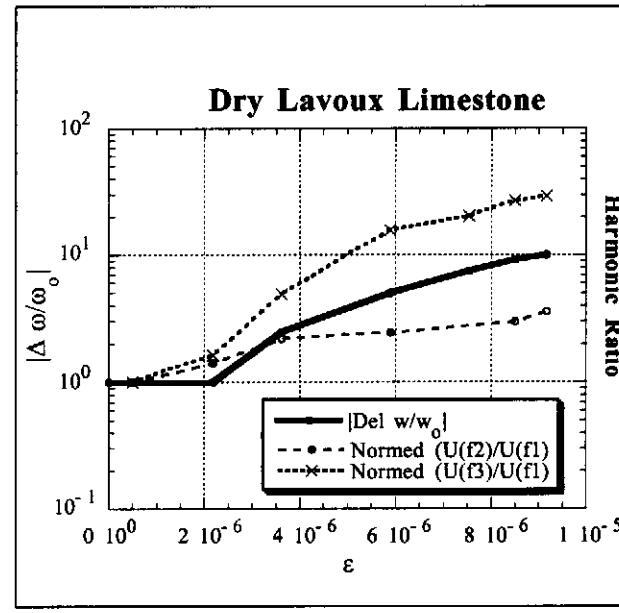

Fig. 13. Change in resonant frequency ($\Delta\omega/\omega_0$) normed to its minimum value $\Delta\omega/\omega_{0min}$ shown by the solid bold line. ω_0 is the unperturbed ("linear") resonant peak and $\Delta\omega = \omega - \omega_0$. The change is measured at the peak resonance response for each frequency sweep as illustrated in Figure 12. Harmonic ratios of the second $[2f_1]$ and third harmonics $[3f_2]$ as a function of the detected strain amplitude ϵ are shown by the dashed lines. The harmonic ratios are normed to their minimum amplitudes (which are virtually identical) at the strain amplitude where the harmonics are first observed, i.e., $\epsilon = 4.9x10^{-07}$. The data are for dry Lavoux limestone.

under resonance conditions for dry Lavoux limestone. The change in resonant frequency ($\Delta\omega/\omega_0$) as a function of the detected strain amplitude is shown by the solid line. The harmonic ratios of the second ($2 \times$ fundamental [$2f_1$]) and third harmonics ($3 \times$ fundamental [$3f_2$]) as a function of detected strain amplitude are shown by the dashed lines. The harmonic ratios are normed to their minimum values which are identical. The amplitude of the third harmonic is clearly larger, and harmonics are observed to appear before an observable resonant peak shift is observed. In general, odd harmonics tend to dominate in amplitude in rock and can be very large at the strain levels studied.

We indicate three fundamental observations that can be regarded as representative for rock. These materials: (1) generally but not always show peak bending (see Johnson et al. (1996); (2) show a rich spectrum of harmonics at strain levels as low as 10^{-7}; and, (3) show a predilection for domination of odd harmonics over even harmonics.

3.4 Dynamic studies of pulsed waves: strain range 10^{-6} to 10^{-9}, frequency range 10^3 to 10^6 Hz

In this set of experiments we illustrate the creation of harmonics along the propagation path for pulse-mode waves at strains ranging from 10^{-6} to 10^{-9} and frequency ranging from 10^3 to 10^6 Hz. Experiment 1 shows results of a single frequency drive for a wave propagating in a bar. Experiment 2 shows results for waves propagating from a broad band input in a similar bar. For a complete description of these experiments see Meegan et al. (1993) and Johnson and McCall (1994).

3.4.1 Pulse-mode apparatus and experimental procedure

The experimental apparatus for pulse-mode measurements is shown in Figure 14. A drive transducer composed of a piezoelectric crystal with a backload was bonded to a 2-m long rod of Berea sandstone. The source transducer was amplified and driven with the desired drive at source displacements from 10^{-9} to 10^{-6} m. In the case of the monofrequency measurements, a single frequency, amplitude modulated wave train was used. Frequencies of 8 to 24 kHz were used for these experiments, but frequencies of 10^3 to 10^6 Hz have been studied in a variety of pulse-mode experiments (e.g., Johnson and Shankland, 1989). Detectors were either embedded in the sample or placed on the sample surface. Care was taken to assure that the measured signals were not contaminated by reflections from the opposite end of the sample. Detected signals were output to a 16 bit waveform analyzer. Experiments were conducted at ambient conditions.

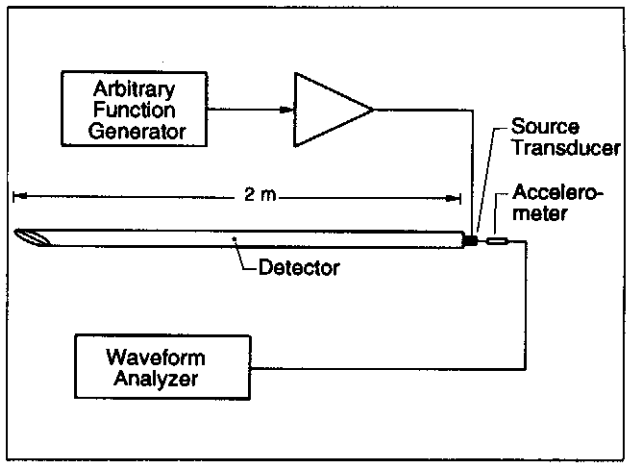

Fig. 14. Experimental apparatus for pulse mode experiments. Either single frequency or arbitrary functions can be input. Detectors are either embedded in the sample or placed on the surface, depending on the experiment.

3.4.2 Experimental observations

A typical experimental observation illustrating harmonic generation for pulsed waves in the rock sample is shown in Figures 15 and 16. Figure 15 shows the frequency spectrum measured at the source for a drive frequency f of 13.75 kHz. The five different curves correspond to five amplitudes of the source transducer varying over a factor of approximately 50. The source displacement spectrum is relatively monochromatic. Figure 16 shows the displacement frequency spectrum at 58 cm, also at increasing drive level. For detected displacements as small as 2×10^{-8} m at the fundamental frequency, the composition of the displacement frequency spectrum at 58 cm is rich in harmonics which are not present at the source. These higher harmonic displacement fields have amplitudes that are a sensitive function of the drive amplitude.

According to classic perturbation theory, the amplitude of the second harmonic is proportional to the propagation distance x. The results in Figure 17 approximately confirms this prediction. Figure 17 illustrates the relative amplitude R of the $2f$ harmonic plotted as a function of distance from the source for a 13.75 kHz drive. The amplitude of the displacement field at $2f$ was found to increase linearly with source - receiver distance x as predicted. The two other predictions from classic theory for $2f$ harmonic behavior in rock with cubic anharmonicity were also approximately confirmed: at fixed x, u_2 scaled as frequency squared (f^2) and as source amplitude squared (U^2) (see Meegan et al., 1993).

The results in Figure 16 show spectral growth at harmonics higher than 2ω. This suggests that higher order terms (i.e. quartic anharmonicity) in the stress strain relationship may be necessary to give a complete description of nonlinear elastic behavior in rock, or that the theory is not complete. In fact, McCall (1994) and

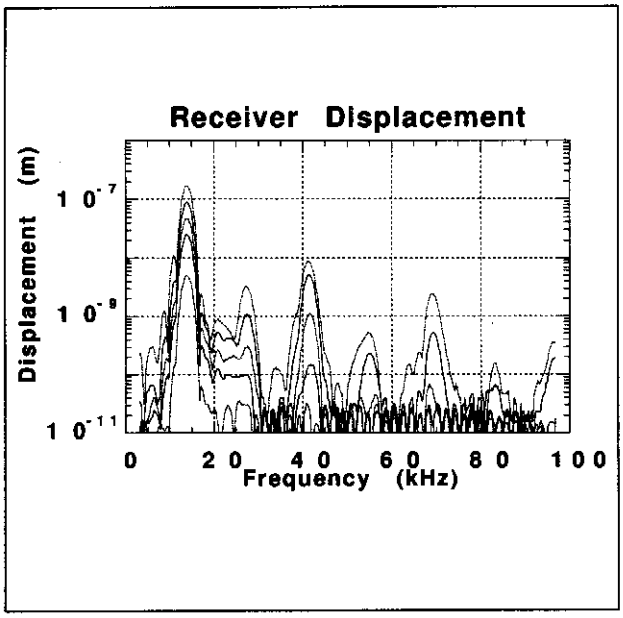

Fig. 15. Source spectra at several drive levels measured for a 13.75 kHz drive.

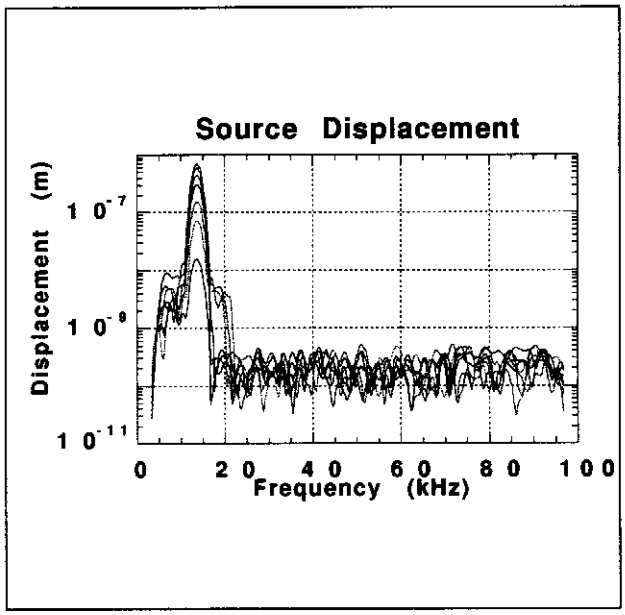

Fig. 16. Detected spectra at 58 cm for the signals shown in Figure 15.

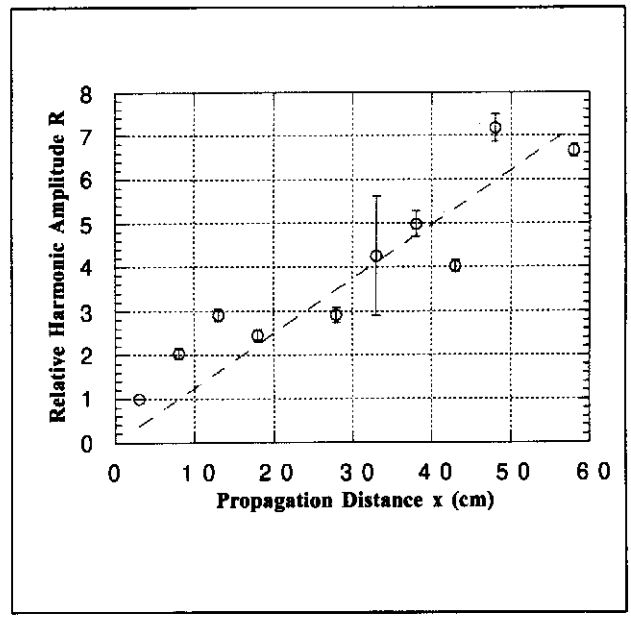

Fig. 17. Dependence of the second harmonic amplitude R on propagation distance x.

Van den Abeele et al. (1995) and Van Den Abeele and Johnson (1996) have included higher order terms in the perturbative solution. In addition, Nazarov et al. (1987) and Guyer et al. (1995a;1995b) and Kadish et al. (1996), among others, have offered models that contain discontinuities in the pressure-density relation. In view of the hysteretic behavior shown in the previous experiments, discontinuous models may ultimately prove to be a more physically realistic approach for modeling of rock.

Figures 18 and 19 show the results for a similar experiment to the above but using a broad-band source. Figure 18 shows the frequency spectrum measured at the source for a drive frequency of 7–32 kHz with peak amplitude at approximately 20 kHz. (The source is a Blackman window). The seven different curves correspond to progressively increasing drive amplitudes varying over a factor of approximately 10^3. The source displacement spectrum contains only a small fraction of harmonic and intermodulation effects and only at large drive levels. Figure 19 shows the resulting displacement frequency spectrum at 1 m. For detected displacements at the fundamental frequency as small as $3\times10^{-}8$ m, the composition of the displacement frequency spectrum at 1 m is extremely rich in frequencies not present at the source. As drive amplitude is increased the spectrum becomes progressively richer due to the nonlinear elastic wave interaction in the material. Harmonic growth is apparent at detector strain levels of less than 10^{-7} in this experiment.

The broadening in the spectrum is due to the fact that a source composed of two frequencies gives rise to waves propagating at harmonics of both source frequencies in addition to waves at the sum and difference frequencies

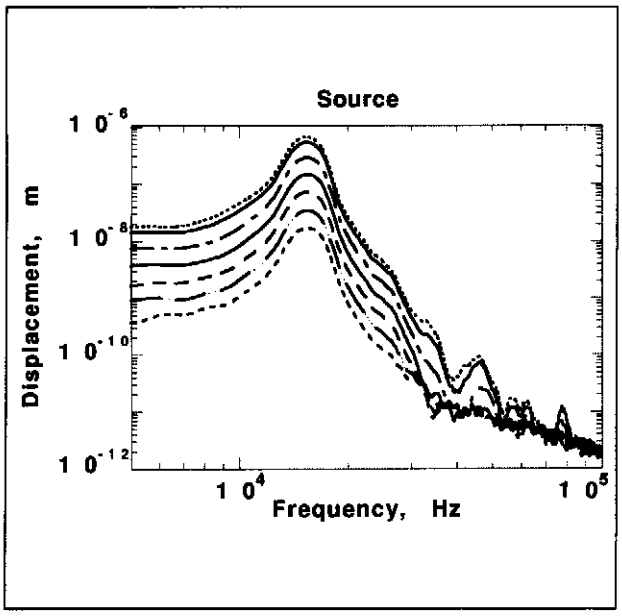

Fig. 18. Source displacement spectrum at increasing applied voltages as shown by the different line types. Drive is a Blackman window with peak at 20 kHz which begins and ends at 7 and 32 kHz, respectively.

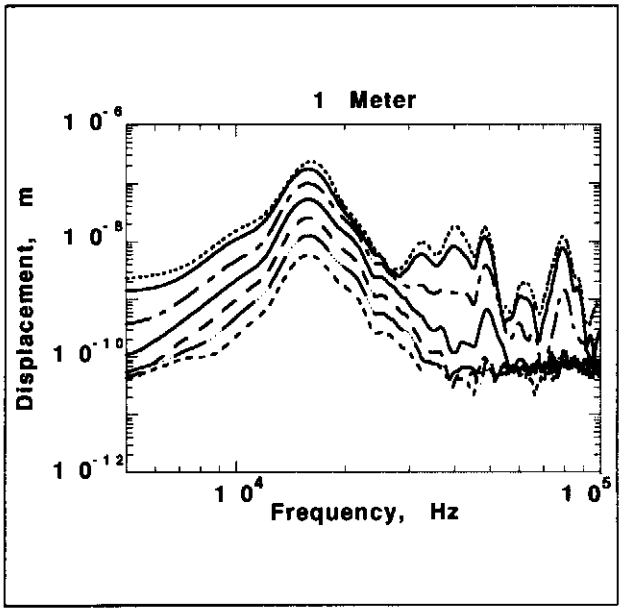

Fig. 19. Displacement spectrum 1 m from source at increasing applied voltages corresponding to drive levels in Figure 18.

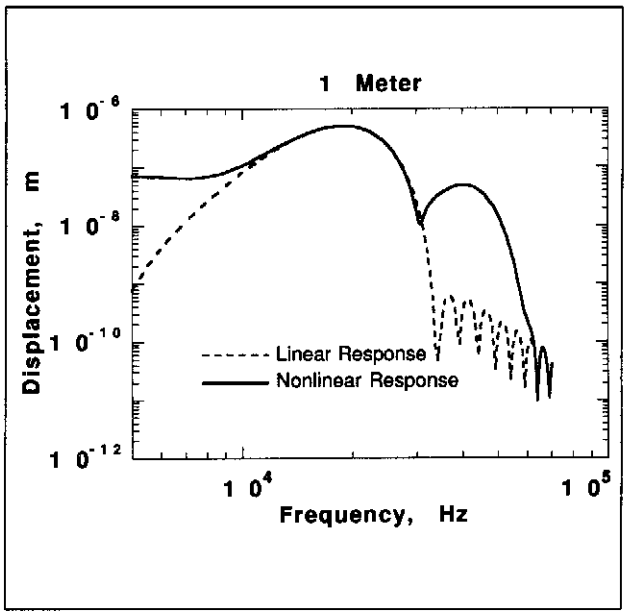

Fig. 20. Model result showing linear response (dashed line) and nonlinear response (solid line) at 1 meter for a drive signal identical to that input to the sample. The model result contains no wave attenuation.

between the two source frequencies. In general, for a source composed of n frequencies, n harmonics will be created. Additionally, each individual frequency will interact with all other frequencies present creating waves at their respective sum and difference frequencies (Note that this experiment is the analogue to that conducted by Pestorious and Blackstock in gas in the early 1970s). Figure 20 shows a theoretical result from classic perturbation theory at one meter. Both the linear response (dashed line) and the "linear plus nonlinear" response (solid line) are shown. In the model $\beta = -10^3$ and contains no dissipation (see Eqs. 1 and 4) . There is good qualitative agreement between the model and the experimental results. The shape of the detected experimental spectrum is influenced by the response of the system including the response of transducers and electronics. This is not a large effect, however, and it is linear with drive amplitude. Again, the presence of higher harmonics than $2f$ suggests that other sources of elastic nonlinearity are important to a complete description of nonlinear elastic behavior in rock.

4 Discussion

4.0.3 Harmonics and study of nonlinear elasticity

The examples from numerous laboratory experiments shown in this paper indicate that nonlinear elastic response is a pervasive characteristic of rock over orders of magnitude in frequency and strain. In geoscience, the nonlinear response of rock has been largely ignored in the past, despite the evidence suggesting the effect is sig-

nificant, especially from numerous published static tests of stress-strain. Pioneering experimental work such as that by Holcomb (1981), Winkler et al. (1978), Murphy (1982) and Bulau and Tittman (1984) and Nazarov et al. (1988) have provided evidence suggesting this was the case. In general, first order effects such as change in modulus or velocity have been commonly employed by numerous researchers at nearly all frequency and strain intervals described here. We argue that in static tests, end point memory and hysteresis should be monitored for study of nonlinear response (not simply the upgoing stress-strain response which is commonly the only response measured). Guyer and McCall (1996), and Guyer et al. (1995a;1995b) show that a complete description of the nonlinear response can be predicted from static hysteresis tests.

In dynamic tests, the second order effects (harmonics) are those that should be monitored. For example, the pulse mode tests shown in Figures 15–20 suggest this: no change in velocity was observed but harmonics were clearly and abundantly generated along the wave propagation path. In general, our experience shows us that nonlinear effects may be observable from study of harmonics before being observed using more established methods.

4.0.4 Mechanism

The primary mechanisms that produce nonlinear response in rock are due to the low-aspect ratio compliant features (gracks, crain-to-grain contacts, etc.) [e.g., see Gist, 1994] and the presence of fluids (see. e.g., Johnson et al., 1996 and Zinszner et al., 1996). Anharmonicity in the solid matrix produces very small contributions. Beyond the primary mechanisms, little work has been conducted to see what the relative contributions are. This work has been initiated by Zinszner et al. (1996). Much more work needs to be done in this area if quantitative applications are to be developed.

4.0.5 Future Research

A fundamental question remains as to the value of measuring and understanding nonlinear elasticity in rock over and above academic interest. To first order, the nonlinear elastic response is certainly related to the micro and macro structure of the material, the grain to grain contacts, the microcracks, joints, etc. The contained fluid also plays an important role based on our experience. The sensitivity of the nonlinear response to the structure and fluid content is far larger than that of standard linear measurements of wave speed, modulus and attenuation. The problem is that these measurements are difficult to make and great care must be taken in separating the apparatus effects that can be identical. These are problems that are surmountable. Many questions remain in regards to additional nonlinear mechanisms, strain rates, extracting results from field data, etc. Ultimately, the rewards of research in this area may be great. We believe that the work presented in this paper and work on nonlinear elasticity by other groups will lead us to a new level of understanding in regards to the makeup of materials.

5. Conclusions

We have demonstrated that nonlinear elasticity is a pervasive characteristic of rocks over strain intervals from 10^{-1} to 10^{-9} and frequency intervals of near dc to the MHz range from laboratory experiments. The ramifications of nonlinear response in rock may ultimately affect many areas of research in Geoscience including seismology, where the spectral distortion of seismic waves during propagation must be considered (e.g., Johnson and McCall, 1994; Bulau et al., 1984). Other areas of research include rock mechanics and materials science where the nonlinear response of a material may be used for characterization purposes. In addition, characterization of material property change by monitoring nonlinear response may be of value. For instance, these changes include variations in water saturation for porous media, change in response to variations in stress, change induced by fatigue damage, etc.

Acknowledgements. This work was supported by the Office of Basic Energy Science of the United States Department of Energy under contracts W-7405-ENG-36 (Los Alamos National Laboratory) with the University of California, and the Institut Français du Pétrole. We thank Bernard Zinszner, Thomas Shankland, Brian Bonner, R. J. O'Connell, Albert Migliori, Igor Beresnev, Koen Van Den Abeele, T. V. McEvilly, V. Korneev, Kurt Nihei, Abe Kadish, Brun Hilbert, and James Ten Cate for helpful discussions. We are indebted to Koen Van Den Abeele, Robert Guyer, Katherine McCall for constructive review of the manuscript.

References

Bakulin V. N., and Protosenya, A. G., Nonlinear effects in travel of elastic waves through rocks, Transactions (Doklady) of the USSR Academy of Sciences, Earth Sciences Sections , 263, 314-316, 1981.

Beresnev, I. A. and Nikolaev, A. V., Experimental investigations of nonlinear seismic effects, Phys. of the Earth and Planetary Int., 50, 83-87, 1988.

Birch, F., in Handbook of Physical Constants, Clark, S. P. , Jr. (Ed.) Geol. Soc. Am. Press, Connecticut, 97-174, 1966.

Bonner, B. P. and Wanamaker, B. J., in Review of Progress in Quantitative NDE, Thompson, D. O., and Chimenti, D. E. (Eds.), Plenum, New York and London, 9B, 1709-1712 , 1990.

Bonner, B. P. and Wanamaker, B. J., Acoustic nonlinearities produced by a single macroscopic fracture in granite, in Review of Progress in Quantitative NDE, Thompson, D. O., and Chimenti, D. E. (Eds.), Plenum, New York and London, 10B, 1861-1867, 1991.

Bulau, J. R., Tittmann, B. R., and Abdel-Gawad, M., Nonlinear wave propagation in rock, Proceedings of the 1984 IEEE Ultrasonics Symposium, 775-780, 1984.

Gist, G. A., Fluid effects on velocity and attenuation in sandstones, J. Acoust. Soc. Am. 96 (2) 1158-1173, 1994.

Guyer, R. A. and McCall, K. R., Hysteresis, discrete memory and nonlinear elastic wave propagation in rock: a new paradigm, Nonlinear Processes in Geophysics, in press, 1996.

Guyer, R. A., McCall, K. R., and Boitnott, G. N., Hysteresis, discrete memory and nonlinear wave propagation in rock, Phys. Rev. Let., 74, 3491-3494, 1995a.

Guyer, R. A., McCall, K. R. , Johnson, P. A., Rasolofosaon, P. N. J., and Zinszner, B., Equation of state hysteresis and resonant bar measurements on rock, 35th U. S. Symposium on Rock Mechanics, Daemen, J. J. K. and Schultz, R. A. (Eds.) Balkema, Rotterdam, 177-181, 1995b.

Hilbert, L. B., Jr., Hwong, T. K. ,Cook, N. G. W. , Nihei, K. T., and Myer, L R., Effects of strain amplitude on the static and dynamic nonlinear deformation of Berea sandstone, Rock Mechanics Models and Measurements: Challenges From Industry, Nelson, P. P., and Laubach, S. E. (Eds.) Balkema, Rotterdam, 497-504, 1994.

Holcomb, D. J., Memory, relaxation, and microfracturing in dilatant rock, J. Geophys. Res., 86, 6235, 1981.

Johnson, P. A. and McCall, K. R., Observation and implications of nonlinear elastic wave response in rock, Geophys. Res. Lett. 21, 165-168, 1994.

Johnson, P. A., Shankland, T.J., O'Connell, R.J., and Albright, J.N., Nonlinear generation of elastic waves in crystalline rock, J. Geophys. Res., 92, 3597-3602, 1987.

Johnson, P. A. and Shankland, T. J. Nonlinear generation of elastic waves in granite and sandstone: continuous wave and travel time observations, J. Geophys. Res. 94, 17,729-17,733 , 1989.

Johnson, P. A., Zinszner, B., Rasolofosaon, P. N. J., Resonance and elastic nonlinear phenomena in rock, J. Geophys. Res., in press, 1996.

Kadish, A. , Johnson, P. A., and Zinszner, B., Evaluating hysteresis in earth materials under dynamic resonance, J. Geophys. Res., in press, 1996.

Landau, L. D. and Lifshitz, E. M., Theory of elasticity, 3rd edition, Pergamon Press, Oxford, 1986.

Liu, F., Nonlinear Elasticity, seismic anisotropy and petrophysical properties of reservoir rocks, Ph.D. Dissertation, Stanford University, 1994.

McCall, K. R. and Guyer, R. A., Equation of state and wave propagation in hysteretic nonlinear elastic material, J. Geophys. Res., in press, 1994.

McCall, K. R., Theoretical study of nonlinear acoustic wave propagation, J. Geophys. Res. 99, 2591-2600, 1993.

Meegan, G. D., Johnson, P. A., Guyer, R. A.. and McCall, K. R., Observations of nonlinear elastic wave behavior in sandstone, J. Acoust. Soc. Am. 94, 3387-3391, 1993.

Murphy, W. F. III, Ph.D. Dissertation, Stanford University, 1982.

Nazarov, V. E., Ostrovsky, L. A., Soustova, I. A., and Sutin, A. M., Nonlinear acoustics of micro-inhomogeneous media, Phys. Earth and Planet. Int., 50, 65-73, 1987.

Ostrovsky, L. A., Wave processes in media with strong acoustic nonlinearity, J. Acoust. Soc. Am., 90, 3332-3337, 1991.

Ostrovsky, L. A., Nonlinear dynamics of media with complex structures, Dynamics of Systems 1, 115-130 (a publication by the Nizny Novgorod branch of the Blagonravov Inst. of Machinery of the Russian Acad. Sci.), 1993.

Stoker, J. J., Nonlinear Vibrations in Mechanical and Electrical Systems, Interscience Publishers, Inc., New York, 1950.

Toksöz, M. N., and Johnston, D. H., Definitions and terminology, in Seismic Wave Attenuation, Society of Exploration Geophysicists Geophysics Reprint Series No. 2, Johnston, D. H. and Toksöz, M. N. (Eds.) SEG Tulsa, 1981.

Van Den Abeele, K. E-A., TenCate, J. A. , Guyer, R. A. , McCall, K. R. , Johnson, P. A., and Shankland, T. J., Extreme nonlinearity in rocks: an investigation using elastic pulse wave propagation, Proceedings of the 1995 International Congress on Acoustics I, Newman, M. (Ed), 193-196, 1995.

Van Den Abeele K. and Johnson P.A. Elastic pulsed wave propagation in media with second or higher order Nonlinearity. Part II: simulation of experimental measurements on Berea sandstone, J. Acoust. Soc. Am., in press, 1996.

Winkler, K., Nur, A., and Gladwin, M., Friction and seismic attenuation in rocks, Nature, 277, 528-531, 1979.

Zinov'yeva, G. P., Nesterov, I. I., Zdhakhin, Y. L., Artma, E. E., and Gorbunov, Y. V., Investigation of rock deformation properties in terms of the nonlinear acoustic parameter, Transactions (Doklady) of the USSR Academy of Sciences, Earth Science Sections 307, 337-341, 1989.

Zinszner, B., Johnson, P. A., and Rasolofosaon, P. N. J., Influence of change in physical state on elastic nonlinear response in rock: effects of confining pressure and saturation, J. Geophys. Res., in review, 1996.